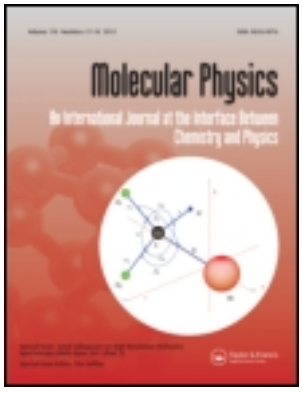

Molecular Physics: An International Journal at the Interface Between Chemistry and Physics
Publication details, including instructions for authors and subscription information:
http://www.tandfonline.com/loi/tmph20

Evolution of geometrical structures, stabilities and electronic properties of neutral and anionic $Li_n Cu^{\lambda}$ (n=1-9, λ=0, -1) clusters: compare with pure lithium clusters

Peng Shao [a], Xiao-Yu Kuang [a], Li-Ping Ding [a], Ming-Min Zhong [a] & Zhen-hua Wang [a a]
[a] Institute of Atomic and Molecular Physics, Sichuan University, Chengdu 610065, China
Accepted author version posted online: 05 Oct 2012.Published online: 24 Oct 2012.

To cite this article: Peng Shao , Xiao-Yu Kuang , Li-Ping Ding , Ming-Min Zhong & Zhen-hua Wang (2013) Evolution of geometrical structures, stabilities and electronic properties of neutral and anionic $Li_n Cu^{\lambda}$ (n=1-9, λ=0, -1) clusters: compare with pure lithium clusters, Molecular Physics: An International Journal at the Interface Between Chemistry and Physics, 111:4, 569-580, DOI: 10.1080/00268976.2012.737036

To link to this article: http://dx.doi.org/10.1080/00268976.2012.737036

Molecular Physics, 2013
Vol. 111, No. 4, 569–580, http://dx.doi.org/10.1080/00268976.2012.737036

Taylor & Francis
Taylor & Francis Group

RESEARCH ARTICLE

Evolution of geometrical structures, stabilities and electronic properties of neutral and anionic Li_nCu^{λ} ($n = 1$–9, $\lambda = 0, -1$) clusters: compare with pure lithium clusters

Peng Shao, Xiao-Yu Kuang*, Li-Ping Ding, Ming-Min Zhong and Zhen-hua Wang

Institute of Atomic and Molecular Physics, Sichuan University, Chengdu 610065, China

(*Received 6 September 2012; final version received 25 September 2012*)

The structural evolution, stabilities, and electronic properties of copper-doped lithium Li_nCu^{λ} ($n = 1$–9, $\lambda = 0, -1$) clusters have been systematically investigated using a density functional method at PW91PW91 level. Extensive searches for ground-state structures were carried out, and the results showed the copper tends to occupy the most highly coordinated position and form the largest probable number of bonds with lithium atoms. By calculating the binding energies per atom, fragmentation energies and the HOMO-LOMO gaps, we found LiCu, Li_7Cu, $LiCu^-$, Li_2Cu^- and Li_8Cu^- clusters have the stronger relative stability and enhanced chemical stability. The content and pattern of frontier MOs for the most stable doped isomers were analysed to investigate the bond nature of interaction among Li and Cu atoms. The results show some σ-type and π-type bonds are formed among them, and with small admixture of the Cu *d* characters. To achieve a deep insight into the electron localization and reliable electronic structure information, the natural population analysis and electron localization function were performed and discussed.

Keywords: Density functional theory; Cu-Li cluster; structural properties; electron localization function

1. Introduction

In the last few decades, metallic clusters have received great interest from physicists and quantum chemists due to their potential application in catalytic processes, materials science, biology, and medicine [1–5]. A very intriguing example of such properties is the claimed occurrence of exceptionally large abundances for some cluster sizes detected during cluster preparation (so-called 'magic' numbers). The 'magic' numbers can be predicted by the jellium model [6–8]. This model predicts that clusters with closed-shell electronic configurations are particularly stable. Thus, clusters with 2, 8, 20, 40 . . . electrons can close $1s^2$, $1p^6$, $1d^{10}$, $2s^2$, $1f^{14}$, $2p^6$ . . . shells, respectively, and in analogy with nuclear shell structure should be very stable. This model has been most successful in describing the electronic structure of alkali metal cluster, which may be due to the alkali systems have free-electron nature. Among them, lithium clusters are deceptively simple. Although lithium has only three electrons, the highly diffusive nature of the bound electron and the multi-configurational nature of the wave-functions for the neutral clusters lead to numerous complications, [9,10] making results sensitive to choose the computational methodology and basis sets. On the other hand, they have small masses, which make them difficult to decelerate in photoelectron spectroscopic experiments. These characteristics make the lithium cluster represent a challenge for both experimental and theoretical studies. Thus, it is not surprising that there are only a few reported studies on anionic lithium clusters [11–19].

Early research to understand small neutral and cationic lithium clusters was undertaken by Boustani *et al.* [20] who found that very small Li_n ($n \leq 6$) clusters prefer planar geometries and the optimal geometries of somewhat larger Li_n ($6 \geq n \leq 9$) clusters are composed from condensed deformed tetrahedra. Photoelectron spectra of alkali tetramers were reported in 1995, [21] and it showed that Li_4^- has an anomalous photoelectron spectrum as compared with all other alkali tetramers. Lithium clusters of 2–40 atoms have been studied using density functional theory (DFT) with both local density approximation (LDA) [22–24] as well as nonlocal gradient-corrected functionals. [21,22,23] Very recently, Alexandrova and her co-workers [9] report the results of the systematic joint theoretical and photoelectron spectroscopic study of the Li_n^- ($n = 3$–7) clusters. Their work mainly contributes to the general understanding of the properties and electronic structure of small anion lithium clusters.

*Corresponding author. Email: scu_kxy@163.com

Table 1. Calculated values of bond length r (Å), dissociation energy D_e (eV), frequency ω_e (cm^{-1}) for the LiCu, Li_2 and Li_2^- molecules at different level.

	LiCu			Li_2			Li_2^-		
Methods	r(Å)	D_e(eV)	$\omega_e(cm^{-1})$	r(Å)	D_e(eV)	$\omega_e(cm^{-1})$	r(Å)	D_e(eV)	$\omega_e(cm^{-1})$
B3LYP	2.27	1.83	384.36	2.71	0.90	341.00	3.09	0.86	214.73
B3PW91	2.30	1.66	375.03	2.74	0.80	335.56	3.13	0.89	213.36
BPW91	2.27	1.83	391.88	2.75	0.77	326.88	3.12	0.89	213.81
B3P86	2.28	1.82	386.00	2.71	0.89	343.8	3.10	0.92	218.01
CCSD (T)	2.37	1.80	352.96	2.72	0.91	328.35	3.15	0.88	210.55
PW91PW91	2.26	2.01	398.95	2.73	0.92	329.8	3.09	0.98	220.39
Exp.	2.26[a]	1.95[c], 1.96[b]	465.9[c]	2.67[c]	1.05[c]	351.4[c]	3.09 ± 0.015[d]		232 ± 35[d]

[a]Ref. 41, [b]Ref. 44, [c]Ref. 45, [d]Ref. 46

It can be well established that an impurity doped into clusters can lead to fundamental changes in their geometries, energy properties, and bonding nature, leading to new materials. The main interest in studying heterogeneous lithium clusters is the transformation from a partly ionic bonding in small clusters to the limit of delocalized electrons in the bulk metal. The heterogeneous clusters doped by boron Li_nB, [25] aluminum Li_nAl, [26] beryllium Li_nBe, [27] magnesium Li_nMg, [28] sodium Li_nNa, [29] germanium Li_nGe, [30] and tin Li_nSn [31] have been investigated theoretically. Alexandrova and her co-workers performed a report on the appearance of covalency in Li-doped metal clusters recently. [32,33] Meanwhile, some relevant experimental information is also performed by some groups. The small size heterogeneous lithium clusters of type Li_nX, *i.e.* Li_3O, Li_4O, Li_6C, Li_3S, Li_4S, Li_4P, Li_2CN, Li_nH ($n = 1$–4) [34–39] were investigated in equilibrium vapor of solid or liquid samples by Knudsen-effusion mass spectrometry combined with the electron impact ionization. In a class of Li_nI ($n \geq 2$) clusters, experimental investigations have confirmed the existence of dilithium iodide (Li_2I) which was detected in a mass spectrometer using a Knudsen effusion cell [40]. Russon *et al*. extend the studies of the interaction between main group metals and transition metals by investigating the spectroscopy of diatomic LiCu, [41] which provides a model for the interaction between lithium and transition metals. The copper has the stable $3d^{10}4s^1$ configurations, while the lithium atom has the same s^1 valence configuration. The limited number of valence electrons greatly simplifies theory and spectroscopy on resulting metal dimers due to the low density of excited molecular electronic states [42,43]. It is expected that the combination of a Cu atom with a Li atom will result in a simple *s*-*s* σ bond.

However, to the best of our knowledge, no systematical theoretical studies for copper doped lithium cluster have been found. Therefore, we reported a more extensive and systematical density functional theory investigation on the small sized neutral and anionic Li_nCu^{λ} ($n = 1$–9; $\lambda = 0, -1$) clusters. The main objective of this research is to investigate the nature of interaction between lithium and copper atoms, meanwhile, to compare our extensive computational results with previous experimental findings. [41, 44–46] The various ground-state structures for Li_nCu^{λ} ($n = 1$–9; $\lambda = 0, -1$) are also obtained, which can provide significant help for such cluster assembled materials.

2. Computational methods

Geometrical structures optimizations and frequency analysis of Li_nCu^{λ} ($n = 1$–9, $\lambda = 0, -1$) clusters have been performed by the density functional theory (DFT) method using the *GAUSSIAN 03* program [47] with the (Perdew/Wang 91) PW91PW91 [48] functional. The PW91PW91 model allows obtaining remarkable results both for covalent and noncovalent interactions in a quite satisfactory theoretical framework encompassing the free electron gas limit and most of the known scaling conditions. In order to choose the suitable computational method and basis set to describe our systems, we calculated the bond lengths, dissociation energies and vibrational frequencies of Li_2^-, Li_2, and LiCu dimers. The results which compared with the experimental values are summarized in Tables 1. First, we wanted to calculate the Li–Cu system employing the CCSD(T) method and all-electron basis set, while the calculated bond length of LiCu is 2.14 Å, which is far from the experimental value (2.26 Å). The bond lengths, dissociation energies and vibrational frequencies of Li_2^- and Li_2 also discouraged us to choose this method and basis set. After a series of tests, the results based on PW91PW91/GENECP level were tested to be in good agreement

with the experimental values. This indicates the suitability of current computational method and basis set. The basis sets labeled GENECP are the combinations of LanL2DZ [49–51] and 6-311 + G [52,53] basis sets, which are employed for the Cu and Li atom, respectively.

To search for the lowest energy structure of copper-doped lithium clusters, the equilibrium geometries of bare lithium clusters were first studied. It is well known that the pure lithium clusters in the range 2–10 atoms have been well studied. We searched the pure neutral and anionic lithium clusters by considering all the possible structures reported in previous papers [9,17,19,20,54] and the results in this work agree well with those obtained by global minimum optimization [9,19]. Then a large number of isomeric structures of copper-doped lithium clusters were obtained by placing the Cu atom on each possible site of the $Li_n^{0/-}$ host clusters as well as by substituting one Li atom using Cu in $Li_{n+1}^{0/-}$ clusters. Due to the spin polarization, every initial structure is optimized at various possible spin multiplicities. It is worth pointing out that all of the clusters are found to prefer the lowest spin state. In order to confirm that the optimized geometry corresponds to a local minimum in potential energy, each of them is followed by a harmonic vibrational frequencies analysis. In this way, a large number of optimized isomers for Li_nCu^{λ} ($n = 1$–9, $\lambda = 0, -1$) clusters are obtained, but here we only list a few energetically low-lying isomers for each size in Figure 1 and 2. Meanwhile, the isomers of the ground-state $Li_n^{0/-}$ ($n = 2$–10) cluster are also displayed for comparison. We believe that we have identified the geometrical structures of small size bare lithium clusters and copper-doped lithium clusters correctly. This belief is based on our ability to explain the relative stabilities, orbital analysis, and electronic properties consistently and quantitatively.

3. Results and discussion

3.1. *Geometrical structures*

The starting point in any description of cluster properties is their geometrical structures. Based on the method that has been pointed out above, a large number of optimized isomers for Li_nCu^{λ} ($n = 1$–9, $\lambda = 0, -1$) clusters are obtained. We only select the few energetically low-lying isomers for each size and list them in Figure 1 and 2, respectively. According to their energies from low to high, the neutral isomers are designated by nN-a, nN-b, nN-c, and nN-d; the anions are designated by nA-a, nA-b, nA-c, and nA-d. Where n represents the number of Li atoms in $Li_nCu^{0/-}$ clusters. Meanwhile, in order to examine the effects of dopant Cu atom in lithium clusters, geometry optimizations of $Li_n^{0/-}$ ($n = 2$–10) clusters have been carried out using the identical method and basis set, and the lowest-energy structures are also displayed for comparison. Furthermore, the corresponding relative energies, symmetries, electronic states, HOMO energies, and LUMO energies for the selected pure and doped clusters are summarized in Table 2.

3.1.1. *Bare lithium clusters* $Li_n^{0/-}$ *($n = 2$–10)*

A variety of Li_n and Li_n^- structures were constructed starting from isomers reported in previous studies, and additional new isomers were also studied. For the smallest clusters Li_2 and Li_2^-, the ground states are calculated to be $^1\Sigma_g$ and $^2\Sigma_u$, respectively. These results agree well with previous experimental and theoretical studies [9,46,54]. Low-spin neutral structure Li_3 (C_{2v}, $^2B_2$), distorted from D_{3h} symmetry because of the Jahn–Teller effect, is predicted to be ground-state structure. While the linear Li_3^- isomer with $D_{\infty h}$ symmetry and $^2B_2$ electronic state is found to be the global minimum structure. Those are all in consistent with previous studies [55–57]. The ground-state structures of neutral Li_n change from planar to three-dimensional (3D) structure at $n = 6$, while this transition occurs at $n = 4$ for anionic clusters. Many years ago, the structures and energetics of Li_6, Li_6^- and Li_6^+ were investigated by Temelso and Sherrill [17] using the high accuracy *ab* initio method. They proposed that the D_{4h} isomer is the most stable structure for neutral and anionic Li_6 cluster, which is in agreement with our calculated result. The ground state structure of anionic clusters is dissimilar to those of neutral clusters. This indicates that attachment of an extra electron can exert a great influence on the structure. As shown in Table 2, almost all the neutral and anionic lithium clusters have high symmetry. This may be due to the lithium is a typical metal with deficient metallic bonding.

3.1.2. *Li_nCu^{λ} ($n = 1$–9, $\lambda = 0, -1$) clusters*

The ground-state structures and some low-lying isomers for Li_nCu^{λ} ($n = 1$–9, $\lambda = 0, -1$) clusters are listed in Figure 1 and 2. As expected, the ground state of LiCu is shown to be $^1\Sigma$, with a $3d_{Cu}^{10}\sigma^2$ molecular configuration correlating to the Li ($1s^2 2s^1$, ^2S) + Cu ($3d^{10}4s^1$, ^2S) atomic ground states. The bond length and dissociation energies of LiCu dimer were calculated to be 2.26 Å and 2.01 eV, respectively, which are in good agreement with the values obtained in previous experimental investigation. [41,44,45] When the LiCu dimer attach an extra electron, the ground state of

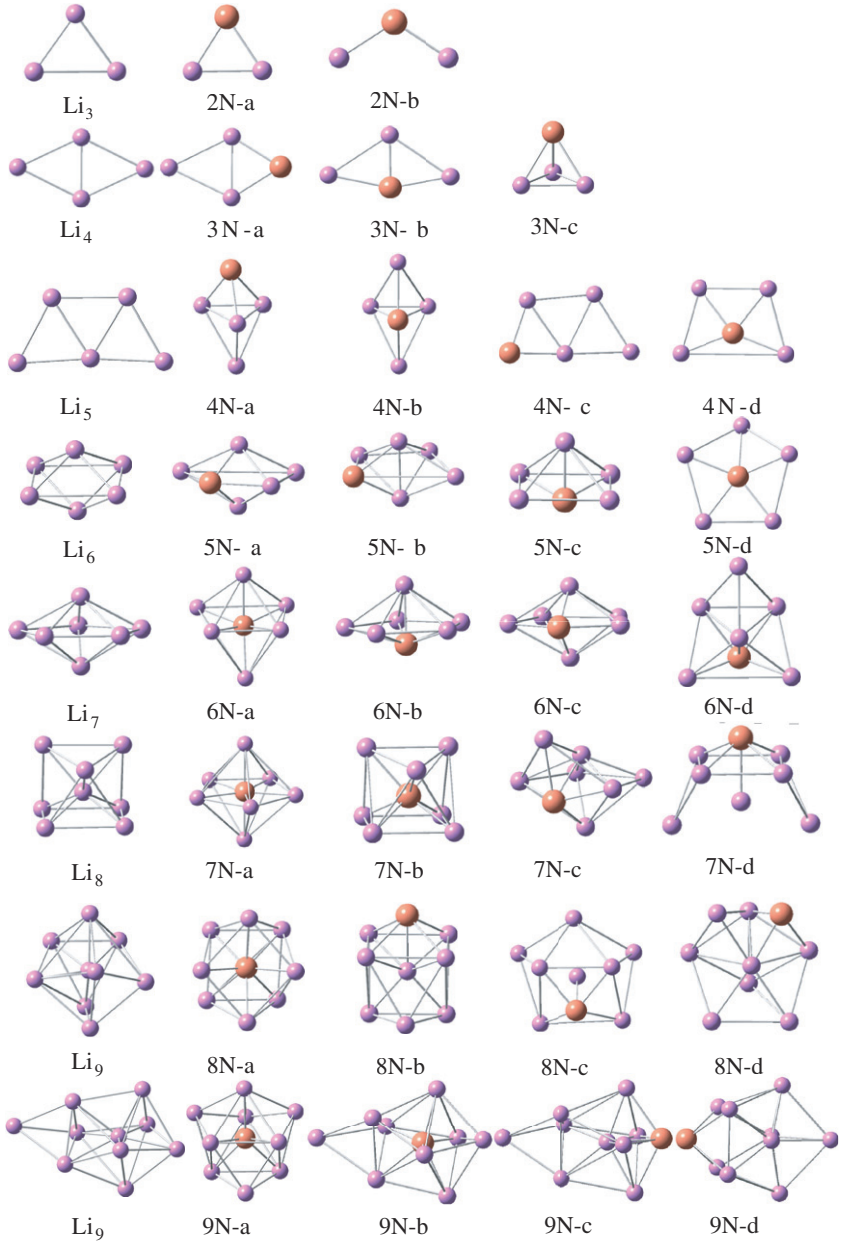

Figure 1. The ground-state structures of Li_{n+1} and Li_nCu ($n=2-9$) clusters, and some low-lying isomers for doped clusters.

anion $LiCu^-$ will change to be $^2\Sigma$, and the bond length is elongated to 2.45 Å. Unfortunately, there are no available experimental values for comparison for anionic $LiCu^-$ dimer up to now, and our theoretical results need to be further verified by experiments. All possible initial structures of $Li_2Cu^{0/-}$ clusters, i.e. linear structures ($D_{\infty h}$, $C_{\infty v}$), and triangle structures (acute angle or obtuse angle) are optimized at PW91PW91 level with different spin multiplicities. The triangle structure (2N-a) with acute angle is found to be the most stable isomer for neutral cluster, while the ground-state isomer of anion is a linear structure (2A-a). Both of them can be obtained by replacing one Li atom by Cu in the corresponding ground-state $Li_3^{0/-}$ clusters. If you take a good look at Figure 1 and 2, you will find the lowest energy isomer 3N-a, 5N-a, 7N-a, 8N-a, 4A-a, 5A-a and 6A-a, including some low-lying isomers, are also obtained by this method. These indicate Cu-substituted $Li_{n+1}^{0/-}$ clusters are the dominating growth pattern for the $Li_nCu^{0/-}$ clusters. Starting at $n=4$, the lowest energy structures of neutral and anionic Li_nCu clusters begin to show appearance of

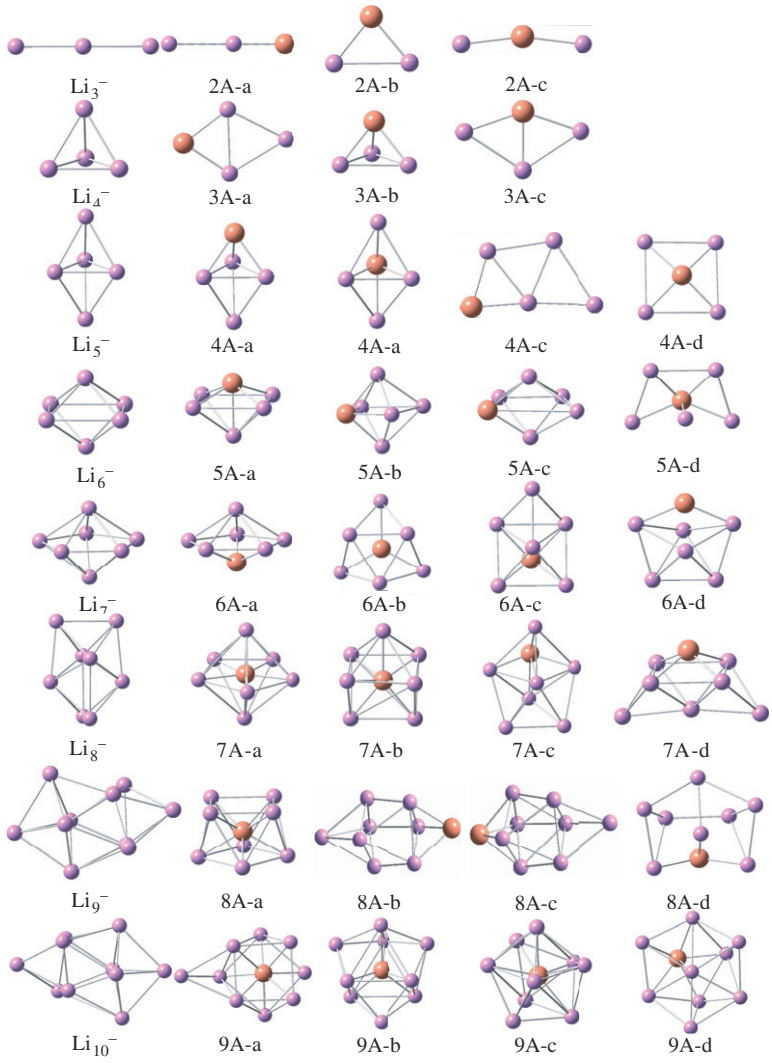

Figure 2. The ground-state structures of Li_{n+1}^- and Li_nCu^- ($n=2$–9) clusters, and some low-lying isomers for doped clusters.

3D geometries. When the number of lithium atoms is up to 5, no low-lying planar structure are found in our calculations. As for 6N-a, 7N-a, 8N-a, 9N-a, 7A-a, 8A-a and 9A-a, the ground state structures consist of two atomic shells, and the inner one being just one copper atom. The copper tends to occupy the centre side and forms the largest probable number of bonds with lithium atoms.

3.2. *Relative stabilities*

In order to investigate the relative stabilities of the ground state Li_nCu^{λ} ($n=1$–9, $\lambda=0$, -1) clusters, we have calculated the binding energies per atom $E_b(n)$ and fragmentation energies $\Delta E(n)$. Considering the influence of impurity atom on the small pure clusters, all of above calculations are compared with the pure Li_{n+1}^{λ} ($n=1$–9, $\lambda=0$, -1) clusters. For Li_nCu^{λ} ($\lambda=0$, -1) clusters, $E_b(n)$ and $\Delta E(n)$ are defined as the following formula:

$$E_b(n) = \left[E\left(Cu^{\lambda}\right) + nE(Li) - E\left(Li_nCu^{\lambda}\right)\right]/(n+1), \quad (1)$$

$$\Delta E(n) = E\left(Li_{n-1}Cu^{\lambda}\right) + E(Li) - E\left(Li_nCu^{\lambda}\right), \quad (2)$$

where $E(Li)$, $E(Cu^{\lambda})$, $E\left(Li_nCu^{\lambda}\right)$ and $E\left(Li_{n-1}Cu^{\lambda}\right)$ denote the total energies of Li, Cu^{λ}, Li_nCu^{λ} and $Li_{n-1}Cu^{\lambda}$ clusters, respectively.

For Li_{n+1}^{λ} ($\lambda=0$, -1) clusters, $E_b(n)$ and $\Delta E(n)$ are defined as follows:

$$E_b(n+1) = \left[E(Li^{\lambda}) + nE(Li) - E\left(Li_{n+1}^{\lambda}\right)\right]/(n+1), \quad (3)$$

$$\Delta E(n+1) = E\left(Li_n^{\lambda}\right) + E(Li) - E\left(Li_{n+1}^{\lambda}\right), \quad (4)$$

Table 2. Electronic states, symmetries, relative energies (ΔE), HOMO energies, LUMO energies, and the vibration frequencies with most IR intensities of Li_n^{λ} and Li_nCu^{λ} ($n = 2$–9; $\lambda = 0, -1$) clusters.

Isomer	State	Sym.	ΔE (eV)	HOMO (eV)	LUMO (eV)	Isomer	State	Sym.	ΔE (eV)	HOMO (eV)	LUMO (eV)
Li_3	**$^2B_2$**	***C_{2v}***	–	**−3.231**	**−1.825**	Li_3^-	**$^1\Sigma_g$**	***$D_{\infty h}$***	–	**0.949**	**1.775**
2N-a	$^2A'$	C_{2v}	0.00	−3.912	−1.940	2A-a	$^1\Sigma$	$C_{\infty v}$	0.00	1.258	2.100
2N-b	$^2A'$	C_{2v}	0.21	−2.757	−2.302	2A-b	$^3B_2$	C_{2v}	0.06	0.029	0.054
						2A-c	$^1A_1$	C_{2v}	0.26	0.025	0.043
Li_4	**$^1\Sigma_g$**	***D_{2h}***	–	**−2.865**	**−2.043**	Li_4^-	**$^4A_1$**	***T_d***	–	**0.425**	**1.223**
3N-a	$^1A'$	C_{2v}	0.00	−2.073	−2.852	3A-a	$^2A'$	C_{2v}	0.00	0.336	1.535
3N-b	$^1A'$	C_{2v}	0.44	−2.774	−2.302	3A-b	$^4A_1$	C_{3v}	0.07	0.019	0.041
3N−c	$^1A_1$	C_{3v}	0.50	−2.709	−2.326	3A-c	$^2A_1$	C_{2v}	0.14	0.018	0.039
Li_5	**$^2A_1$**	***C_{2v}***	–	**−2.914**	**−2.139**	Li_5^-	**$^3A_1$**	***D_{3h}***	–	**0.362**	**0.971**
4N-a	^2A	C_s	0.00	−2.745	−2.413	4A-a	$^3A_1$	C_{3v}	0.00	0.492	−1.100
4N-b	$^2A'$	C_{2v}	0.17	−0.107	−0.088	4A-b	$^3B_1$	C_{2v}	0.14	0.015	0.029
4N-c	^2A	C_s	0.26	−0.113	−0.084	4A-c	$^1A'$	C_s	0.31	0.016	0.039
4N-d	^2A	C_2	0.33	−0.108	−0.081	4A-d	$^1A_1$	C_{4v}	0.37	0.011	0.029
Li_6	**$^1A_{1g}$**	***D_{4h}***	–	**−3.176**	**−2.020**	Li_6^-	**$^2A_{2u}$**	***D_{4h}***	–	**0.237**	**0.716**
5N-a	^1A	C_s	0.00	−2.911	−2.370	5A-a	$^2A_1$	C_{4v}	0.00	0.212	0.645
5N-b	^1A	C_s	0.04	−0.107	−0.087	5A-b	$^2B_1$	C_s	0.03	0.011	0.025
5N-c	$^1A_1$	C_{4v}	0.16	−0.107	−0.094	5A-c	^2A	C_{2v}	0.11	0.013	0.028
5N-d	^1A	C_1	0.19	−0.112	−0.077	5A-d	$^4A'$	C_s	0.34	0.017	0.017
Li_7	**$^2A_2''$**	***D_{5h}***	–	**−2.731**	**−2.272**	Li_7^-	**$^1A_1'$**	***D_{5h}***	–	**0.322**	**0.791**
6N-a	$^2A_1$	C_{3v}	0.00	−3.006	−2.379	6A-a	$^1A_1$	C_{5v}	0.00	0.218	0.701
6N-b	$^2A_1$	C_{5v}	0.01	−0.110	−0.091	6A-b	$^1A_1$	C_{3v}	0.04	0.009	0.025
6N-c	$^2B_1$	D_{2v}	0.05	−0.102	−0.085	6A-c	$^1A'$	C_s	0.16	0.007	0.029
6N-d	$^2A'$	C_s	0.15	−0.111	−0.088	6A-d	^1A	C_{2v}	0.21	0.002	0.027
Li_8	**$^1A'$**	***C_s***	–	**−3.049**	**−1.714**	Li_8^-	**^2A**	***S_4***	–	**0.200**	**0.735**
7N-a	$^1A_1'$	D_{5h}	0.00	−2.935	−2.163	7A-a	$^2A_1'$	D_{5h}	0.00	0.248	0.558
7N-b	$^1A_1$	C_{2v}	0.01	−0.110	−0.079	7A-b	$^2A_1$	C_{2v}	0.01	0.009	0.020
7N-c	$^1A'$	C_s	0.52	−0.107	−0.077	7A-c	$^2A'$	C_s	0.59	0.013	0.027
7N-d	$^1A_1$	C_{2v}	0.56	−0.110	−0.074	7A-d	$^2A_1$	C_{2v}	0.66	0.011	0.022
Li_9	**$^2A_1$**	***D_{2d}***	–	**−2.338**	**−1.953**	Li_9^-	**$^1A'$**	***C_s***	–	**−0.061**	**0.613**
8N-a	^2A	C_2	0.00	−2.666	−2.343	8A-a	$^1A_1$	D_{4d}	0.00	0.108	0.734
8N-b	$^2A'$	C_s	0.94	−0.091	−0.071	8A-b	$^2A'$	C_s	1.01	−0.071	−0.091
8N-c	^2A	C_1	0.97	−0.091	−0.082	8A-c	$^1A'$	C_s	1.05	−0.004	0.023
8N-d	^2A	C_1	1.05	−0.099	−0.083	8A-d	^3A	C_s	2.05	−0.003	0.021
Li_{10}	**$^1A'$**	***C_s***	–	**−2.756**	**−2.039**	Li_{10}^-	**^2B**	***C_2***	–	**0.171**	**0.496**
9N-a	$^1A_1'$	D_{3h}	0.00	−2.833	−2.330	9A-a	$^2A'$	C_s	0.00	0.198	0.532
9N-b	$^1A'$	C_s	0.08	−0.107	−0.076	9A-b	$^4A_1'$	D_{3d}	0.05	0.007	0.019
9N-c	$^1A'$	C_s	0.91	−0.109	−0.075	9A-c	$^4A_1'$	D_{4h}	0.07	0.012	0.013
9N-d	$^1A'$	C_s	0.96	−0.113	−0.086	9A-d	^4A	C_s	0.70	0.001	0.019

where $E(\mathrm{Li})$, $E(\mathrm{Li}^{\lambda})$, $E(\mathrm{Li}_n^{\lambda})$ and $E(\mathrm{Li}_{n+1}^{\lambda})$ denote the total energies of Li, Li^{λ}, Li_n^{λ} and $\mathrm{Li}_{n+1}^{\lambda}$ clusters, respectively.

The values of $E_b(n)$ and $\Delta E(n)$ for the lowest energy $\mathrm{Li}_{n+1}^{\lambda}$ and $\mathrm{Li}_n\mathrm{Cu}^{\lambda}$ ($n = 1$–9, $\lambda = 0, -1$) clusters against the corresponding number of the Li atoms are plotted in Figure 3. The features of size evolution are best viewed and the peaks of curves correspond to those clusters with enhanced local stabilities. For pure Li_{n+1} and Li_{n+1}^- clusters, the binding energies per atom increase gradually with the cluster size increasing, which indicate the stability of $\mathrm{Li}_{n+1}^{0/-}$ is enhanced with the cluster size increasing. The curve of Li_{n+1}^- is higher than those of the corresponding sized Li_{n+1} cluster, reflecting that the stability is also enhanced when the cluster attach an extra electron. As for fragmentation energies, the neutral cluster shows an odd–even alternation phenomenon along with cluster size, while the curve of anion is obtuse angle-like. The visible peak occurs at Li_7 and Li_6^- hinting they are more stable than their neighbouring clusters.

For $\mathrm{Li}_n\mathrm{Cu}^{\lambda}$ ($n = 1$–9, $\lambda = 0, -1$) clusters, the binding energies per atom is significantly higher than those of the corresponding sized pure lithium clusters, reflecting that the interactions between Cu atom and Li_n supply additional energies to the total binding energies.

In other words, the stability of $Li_nCu^{0/-}$ clusters is enhanced when Cu atom is doped into the pure $Li_{n+1}^{0/-}$ clusters. Furthermore, the two curves also increase with the cluster size increasing. Fragmentation energy involves the energy that a Li atom is separated from these clusters. As shown in Figure 3, the fragmentation energies for Li_nCu exhibit strong odd-even oscillations from $n=1$ to 4, and then it increases dramatically and reaches a visible peak at $n=7$. Although the curve of Li_nCu^- is irregular, the obvious peaks occur at $n=1$ and 8. Based on the analysis of binding energies and fragmentation energies, we can know that LiCu, Li_7Cu, $LiCu^-$ and Li_8Cu^- clusters possess dramatically enhanced stability than their neighbouring clusters.

3.3. *Orbital analysis*

The highest occupied-lowest unoccupied molecular orbital (HOMO-LUMO) energy gap, which represents the ability of molecule to participate into chemical reaction in some degree, has been examined. In a sense, it can provide an important criterion to reflect the chemical stability of clusters. A large value of the HOMO-LUMO energy gap is related to an enhanced chemical stability. For the most stable Li_{n+1}^{λ} and Li_nCu^{λ} ($n=1$–9, $\lambda=0$, -1) clusters, HOMO and LUMO energies are listed in Table 2. In addition, the HOMO-LUMO energy gaps against the cluster size are plotted in Figure 4. As shown in Figure 4, the HOMO-LUMO energy gaps of neutral Li_nCu and Li_{n+1} clusters exhibit an odd–even oscillatory behaviour along with cluster size, namely, the clusters with even number of atoms have an enhanced chemical stability due to their larger gaps compared with their neighbours. The odd–even alternation phenomenon is also found for Li_nCu^- clusters, but the feature is opposite. This oscillatory trend can be explained by electron pairing effect. As we all know, both of the Li and Cu atoms have one outermost shell electron. The odd-sized clusters have an even total number of valence electrons and the HOMO is doubly occupied. The electrons in a doubly occupied HOMO have stronger effective core potentials because the electron screening is weaker for electrons in the same orbital than for inner shell electrons. The clusters can more easily acquire an electron in the open-shell HOMO of the system with odd-numbered electrons than in the LUMO of a closed-shell system. That is in contrast to Li_nCu^- clusters which have the opposite features. Furthermore, it was found that there are no apparent even-odd alternation behaviors in Li_{n+1}^- HOMO-LUMO energy gaps. This may indicate that the extra electron can form an electron pair with the outermost shell electron, and exert a great influence on the electronic structure of pure lithium cluster. The remarkable peaks appear at LiCu, Li_2Cu^-, Li_2 and

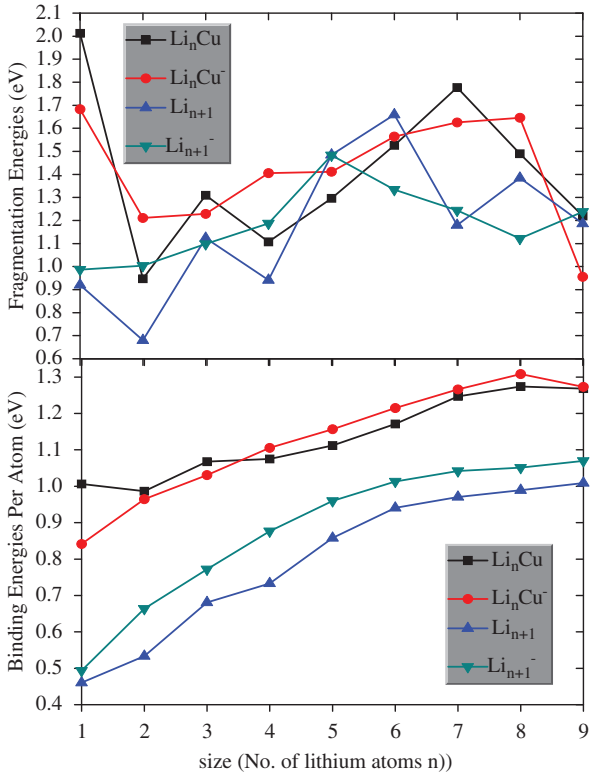

Figure 3. Size dependence of the averaged binding energies$E_b(n)$ and fragmentation energies $\Delta E(n)$ for the ground-state structures of Li_n^{λ} and Li_nCu^{λ} ($n=2$–9; $\lambda=0$, -1) clusters.

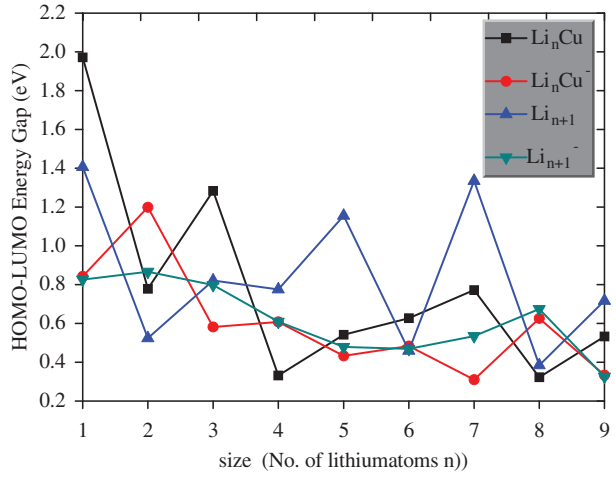

Figure 4. Size dependence of the HOMO-LUMO energy gaps of the ground-state Li_n^{λ} and Li_nCu^{λ} ($n=2$–9; $\lambda=0$, -1) clusters.

Li_8, which imply these clusters possess dramatically enhanced chemical stability.

In order to gain insight into the nature of bonding, we have analysed the content of the highest occupied molecular orbital (HOMO) for ground state isomers. The pattern of frontier MOs for the most stable isomers and some selected pure lithium clusters are displayed in Figure 5. These MOs can provide insight into the observed special features and the nature of bonding between Cu-doped and pure lithium clusters. It is well known that the lithium atom is always *s*-like. As for the HOMO of pure Li_2 clusters, the significant *s* orbital character (97.157%) of Li atom in the frontier orbital is observed. So the σ-type bond is formed between Li and Li atoms. However, when Cu substitutes one Li atom, the σ-type bond disappears but with mixed Cu *d* characters. The σ-type bond is also found in Li_2^- and $LiCu^-$ dimers. For $LiCu^-$, *s*: 51.18% and *p*: 48.81 % of copper atom; *s*: 55.86% and *p*: 44.13 % of Li. In the case of pure Li_6^-, Li_7 and Li_8 clusters, the π-MO is observed. For Li_6^- cluster, the *s*-content decrease to 60.15%, while the *p*-content increase to 39.84%. In the $Li_nCu^{0/-}$ ($n=2$–6) clusters, some σ-type and π-type bonds are formed among the Li and Cu atoms, and with small admixture of the Cu *d* characters. When the number of lithium atoms is up to 7, the ground state structures consist of two atomic shells, and the inner one being just one copper atom. Corresponding to the structure, the frontier MOs also consist of outer and inner atomic shells. The inner one is just an σ-type orbital on copper atom.

3.4. *Electronic properties*

In order to probe into the localization of the charge in ground-state Li_nCu^{λ} ($n=1$–9, $\lambda=0$, -1) clusters and investigate reliable charge-transfer information, the natural population analysis (NPA) for the lowest energy species were calculated and summarized in Table 1 and 4, respectively. As shown in Table 3, it can be clearly seen that the copper atoms in neutral Li_nCu clusters possess negative charges in the range of -0.294 to -3.917 electrons, while most of the Li atoms possess positive charges. This indicates that the electron transfer from the Li_n frames to Cu atom, namely, copper atom acts as electron accepter in all the neutral clusters. This may be due to the electronegativity of Cu (1.90) is much larger than Li (0.98); therefore, the copper has a stronger ability to attract electrons. When an electron is added to the clusters, the copper atoms possess negative charges in the range -0.431 to -3.882 electrons. Compared with the neutral clusters, the charges of copper atoms have little change.

To achieve a deep insight into the reliable electronic structure information, the electron localization function (ELF) was investigated. In quantum chemistry, the ELF is a measure of the likelihood of finding an electron in the neighbourhood space of a reference electron located at a given point and with the same spin. Physically, this measures the extent of spatial localization of the reference electron and provides a method for the mapping of electron pair probability in multielectronic systems. The ELF was originally defined by Axel D. Becke and K. E. Edgecombe in

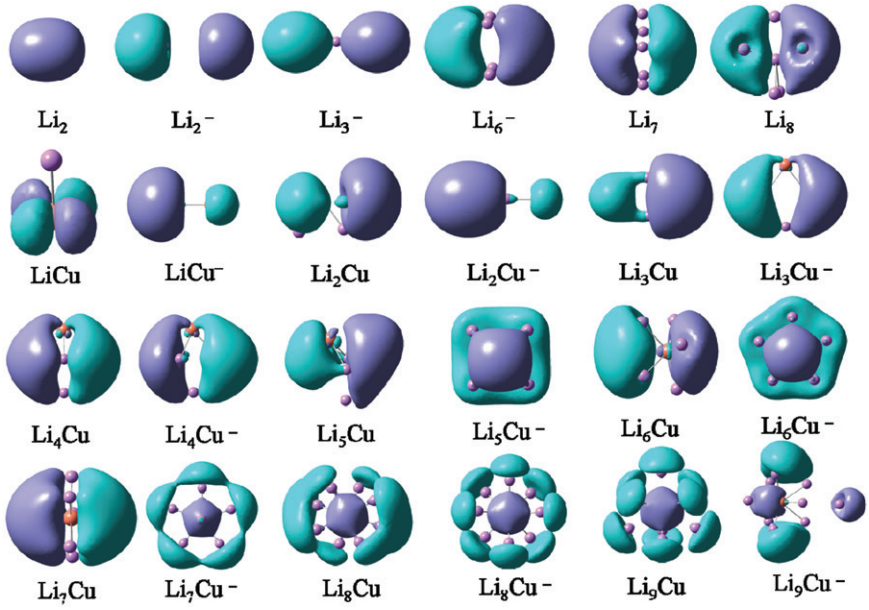

Figure 5. Contour maps of the HOMOs of the ground-state Li_nCu^{λ} ($n=2$–9; $\lambda=0$, -1) and some selected pure lithium clusters.

1990 [58]. They first argued that a measure of the electron localization is provided by:

$$D_\sigma^0(r) = \tau_\sigma(r) - \tfrac{1}{4}\frac{(\nabla\rho_\sigma(r))^2}{\rho_\sigma(r)} \quad (5)$$

where ρ is the electron spin density and τ is the kinetic energy density. And then the electron localization function is defined as follows:

$$ELF = \left(1 + \chi_\sigma^2\right)^{-1} \quad (6)$$

where $\chi_\sigma = D_\sigma(r)/D_\sigma^0(r)$ and $D_\sigma^0(r) = \frac{3}{5}\left(6\pi^2\right)^{\frac{2}{3}}\rho_\sigma^{\frac{5}{2}}(r)\cdot D_\sigma^0(r)$ correspond to a uniform electron gas with spin density equal to the local value of $\rho_\sigma(r)$. The ratio χ_σ is thus a dimensionless localization index calibrated with respect to the uniform-density electron gas as reference. The ELF's possible values are in the range of $0 \le \mathrm{ELF} \le 1$. ELF = 1 corresponds to perfect localization and ELF = ½ corresponds to the electron gas. It means that the ELF shows a clear separation between the core and valence electron, and also shows covalent bonds and lone pairs. The maps for the selected stable clusters (Li_2, LiCu, $LiCu^-$, Li_2Cu^-, Li_3Cu and Li_7Cu) are shown in Figure 6. The ELF analysis of Li_2 show core electron on the two

Table 3. Natural charges populations of the ground-state Li_nCu ($n = 1$–9) clusters. The Al atoms bonding to copper atom denoted are in bold.

isomers	Cu	Li-1	Li-2	Li-3	Li-4	Li-5	Li-6	Li-7	Li-8	Li-9
LiCu	−0.482	**0.482**								
Li_2Cu	−0.464	**0.233**	**0.233**							
Li_3Cu	−0.344	**0.113**	**0.113**	0.118						
Li_4Cu	−0.294	**−0.099**	0.256	0.068	**0.068**					
Li_5Cu	−0.395	0.309	**−0.366**	0.309	**−0.366**	0.472				
Li_6Cu	−2.574	**0.580**	**0.580**	**0.278**	**0.580**	**0.278**	**0.278**			
Li_7Cu	−3.526	**0.573**	**0.476**	**0.573**	**0.476**	**0.476**	**0.476**	**0.476**		
Li_8Cu	−3.581	**0.477**	**0.477**	**0.424**	**0.398**	**0.491**	**0.491**	**0.398**	**0.424**	
Li_9Cu	−3.917	**0.447**	**0.447**	**0.447**	**0.410**	**0.447**	**0.447**	**0.410**	**0.447**	**0.410**

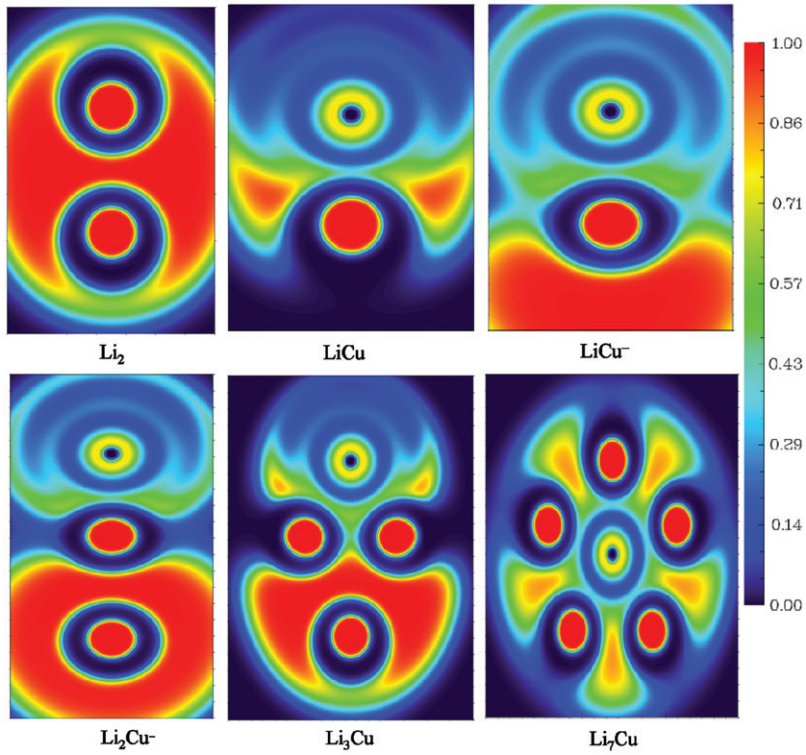

Figure 6. Electron localization function plots of high-stability species Li_2, LiCu, $LiCu^-$, Li_2Cu^-, Li_3Cu and Li_7Cu clusters.

Table 4. Natural charges populations of the ground-state Li_nCu^- ($n = 1$-9) clusters. The Al atoms bonding to copper atom denoted are in bold.

isomers	Cu	Li-1	Li-2	Li-3	Li-4	Li-5	Li-6	Li-7	Li-8	Li-9
$LiCu^-$	−0.673	**−0.237**								
Li_2Cu^-	−0.556	**−0.441**	−0.003							
Li_3Cu^-	−0.462	**−0.222**	**−0.222**	−0.094						
Li_4Cu^-	−0.431	**−0.214**	**−0.214**	0.075	**−0.214**					
Li_5Cu^-	−0.867	**−0.551**	0.104	0.104	0.104	0.104				
Li_6Cu^-	−1.618	0.210	0.210	**−0.433**	0.210	0.210	0.210			
Li_7Cu^-	−3.663	**0.332**	**0.332**	**0.332**	**0.330**	**0.500**	**0.332**	**0.500**		
Li_8Cu^-	−3.882	**0.360**	**0.360**	**0.360**	**0.360**	**0.360**	**0.360**	**0.360**	**0.360**	
Li_9Cu^-	−1.716	**0.123**	**−0.023**	**0.123**	**0.115**	**0.211**	**0.101**	**0.115**	**−0.023**	**−0.026**

lithium atoms. Lots of covalent bond electrons indicate a strong covalent component in the bonding between the two Li atoms. Similar observations are found for LiCu dimer. The covalent bond electrons are associated with the strong Li-Cu bond. It worth pointing out that the calculated ELF values are associated with pseudopotential. In present work, the LANL2DZ effective core potential is chosen to represent the inner-core electrons of Cu atoms. So the core electrons of Cu atoms are not considered during the calculation of ELF. In $LiCu^-$ dimer, the extra electron is in the form of lone pairs below lithium atom. Comparing with LiCu, the covalent bond electrons are decreasing obviously, which indicates the bond nature of interaction in $LiCu^-$ is weaker than that of LiCu cluster. As for Li_2Cu^- and Li_3Cu, there is perfect electron delocalization. The trisynaptic (Li-Li-Li) basins in Li_3Cu indicate the emergence of three-centre–two-electron bonds. The existence of five trisynaptic (Li-Cu-Li) basins confirm the presence of multicentre bonds, and also a global electron delocalization in Li_7Cu that lends further support to its high stability.

4. Conclusions

We predicted the geometrical structures, stabilities, and electronic properties of small pure lithium clusters Li_{n+1}^{λ} and Cu-doped lithium clusters Li_nCu^{λ} ($n = 1$–9, $\lambda = 0, -1$) using density functional theory at the PW91PW91/GENECP level. All the results are summarized as follows.

(a) Extensive searches for possible structures were carried out, and previous global minima are confirmed or new ones identified. The small sized neutral and anionic lithium clusters tend to have high symmetry. For $Li_nCu^{0/-}$ clusters, Cu-substituted $Li_{n+1}^{0/-}$ clusters are the dominating growth pattern. Starting at $n = 4$, the lowest energy structures of neutral and anionic doped clusters begin to show appearance of 3D geometries. The copper atom tends to occupy the most highly coordinated position.

(b) By calculating the binding energies per atom, fragmentation energies and the HOMO-LOMO gaps, we found the LiCu, Li_7Cu, $LiCu^-$, Li_2Cu^- and Li_8Cu^- clusters have the stronger relative stabilities and enhanced chemical stability. The content and pattern of frontier MOs for the most stable doped isomers were investigated. The result show some σ-type and π-type bonds are formed among the Li and Cu atoms, and with small admixture of the Cu *d* characters.

(c) The natural population analysis (NPA) results indicate the electron transfer from Li_n frame to Cu atom in all the neutral clusters, namely, copper atom acts as electron accepter. The electron localization function, which can provide the extent of spatial localization of the reference electron, is also performed for the selected stable clusters.

Acknowledgements

The authors are grateful to the National Natural Science Foundation of China (No. 10974138 and No. 11104190) and the Doctoral Education Fund of Education Ministry of China (No. 20100181110086 and No. 20111223070653).

References

[1] G. Mills, M.S. Gordon and H. Metiu, Chem. Phys. Lett. **359**, 493 (2002).
[2] A.K. Santra and D.W. Goodman, J. Phys. Cond. Mater. **15**, R31 (2003).
[3] R.R. Zope and T. Baruah, Phys. Rev. A **64**, 053202 (2001).

[4] C. Majumder, A.K. Kandalam and P. Jena, Phys. Rev. B **74**, 205437 (2006).
[5] L. Xiao and L. Wang, Chem. Phys. Lett. **392**, 452 (2004).
[6] W.A. deHeer, W.D. Knight, M.Y. Chou and M.L. Cohen, Solid. State. Phys. **40**, 93 (1987).
[7] W. Ekardt, Phys. Rev. Lett. **52**, 1925 (1984).
[8] M. Brack, Rev. Mod. Phys. **65**, 677 (1993).
[9] A.N. Alexandrova, A.I. Boldyrev, X. Li, H.W. Sarkas, J.H. Hendricks, S.T. Arnold and K.H. Bowen, J. Chem. Phys. **134**, 044322 (2011).
[10] J. Simons, J. Phys. Chem. A **112**, 6401 (2008).
[11] H.W. Sarkas, S.T. Arnold, J.H. Hendricks, V.L. Slager and K.H. Bowen, Proc. SPIE **1858**, 240 (1993).
[12] K.K. Sunil and K.D. Jordan, Chem. Phys. Lett. **104**, 343 (1984).
[13] H. Partridge, C.W. Bauschlicher Jr and E.M. Siegbahn, Chem. Phys. Lett. **97**, 198 (1983).
[14] E. Andersen and J. Simons, J. Chem. Phys. **64**, 4548 (1976).
[15] I. Boustani and J. Koutecky, J. Chem. Phys. **88**, 5657 (1988).
[16] H.W. Sarkas, S.T. Arnold, J.H. Hendricks and K.H. Bowen, J. Chem. Phys. **102**, 2653 (1995).
[17] B. Temelso and C.D. Sherrill, J. Chem. Phys. **122**, 064315 (2005).
[18] C.W. Bauschlicher Jr, Chem. Phys. **206**, 35 (1996).
[19] A.N. Alexandrova and A.I. Boldyrev, J. Chem. Theory Comput. **1**, 566 (2005).
[20] I. Boustani, W. Pewestorf, P. Fantucci, V. Bonačić-Koutecký and J. Koutecký, Phys. Rev. **B 35**, 18 (1987).
[21] R. Rousseau and D. Marx, Phys. Rev. **A 56**, 617 (1997).
[22] G. Gardet, F. Rogemond and H. Chermette, J. Chem. Phys. **105**, 9933 (1996).
[23] M.W. Sung, R. Kawai and K.H. Weare, Phys. Rev. Lett. **73**, 3552 (1994).
[24] R.O. Jones, A.I. Lichtenstein and J. Hutter, J. Chem. Phys. **106**, 4566 (1997).
[25] Y. Li, D. Wu, Z.R. Li and C.C. Sun, J. Comput. Chem. **28**, 1677 (2007).
[26] M.S. Lee, S. Gowtham, H. He, K.C. Lau, L. Pan and D.G. Kanhere, Phys. Rev. B **74**, 245412 (2006).
[27] R.Z. Rajendra, T. Baruah and D.G. Kanhere, Phys. Rev. A: At. Mol. Opt. Phys. **63**, 063202 (2001).
[28] M.D. Deshpande, A.J. Dhavale, R.R. Zope, S. Chacko and D.G. Kanhere, Phys. Rev. A: At. Mol. Opt. Phys. **62**, 063202 (2000).
[29] W.L. Cao, C. Gatti, P.J. MacDougall and R.F.W. Bader, Chem. Phys. Lett. **141**, 380 (1987).
[30] V.T. Ngan, J. De Haeck, H.T. Le, G. Gopakumar, P. Lievens and M.T. Nguyen, J. Phys. Chem. A **113**, 9080 (2009).
[31] K. Joshi and D.G. Kanhere, Phys. Rev. A **65**, 043203 (2002).
[32] A.N. Alexandrova, Chem. Phys. Lett. **533**, 1 (2012).
[33] M.T. Huynh and A.N. Alexandrova, J. Phys. Chem. Lett. **2**, 2046 (2011).
[34] H. Kudo, M. Hashimoto, K. Yokoyama, C.H. Wu, A.E. Dorigo, F.M. Bickelhaupt and P.V.R. Schleyer, J. Phys. Chem. **99**, 6477 (1995).
[35] M. Hashimoto, K. Yokoyama, H. Kudo, C.H. Wu and P.V.R. Schleyer, J. Phys. Chem. **100**, 15770 (1996).
[36] H. Kudo, M. Hashimoto, K. Yokoyama, C.H. Wu and P.V.R. Schleyer, Thermochim. Acta **299**, 113 (1997).
[37] H. Kudo and K. Yokoyama, Bull. Chem. Soc. Jpn. **69**, 1459 (1996).
[38] H. Kudo, M. Hashimoto, H. Tanaka and K. Yokoyama, J.Mass Spectrom. Soc. Jpn. **47**, 2 (1999).
[39] S.E. Wheeler, K.W. Sattelmeyer, P.V.R. Schleyer and H.F. Schaefer, J. Chem. Phys. **120**, 4683 (2004).
[40] A. Popovic, L. Bencze and A. Lesar, Rapid Commun. Mass Spectrom. **12**, 917 (1998).
[41] L.M. Russon, G.K. Rothschopf and M.D. Morse, J. Chem. Phys. **107**, 1079 (1997).
[42] M.D. Morse, Chem. Rev. **86**, 1049 (1986).
[43] H.G. Kramer, V. Beutel, K. Weyers and W. Demtroder, Chem. Phys. Lett. **193**, 331 (1992).
[44] A. Neubert and K.F. Zmbov, J. Chem. Soc. Faraday Trans. **I 70**, 2219 (1974).
[45] L.R. Brock, A.M. Knight, J.E. Reddic, J.S. Pilgrim and M.A. Duncan, J. Chem. Phys. **106**, 6268 (1997).
[46] H.W. Sarkas, S.T. Arnold, J.H. Hendricks, V.L. Slager and K.H. Bowen, Z. Phys. D: At., Mol. Clusters **29**, 209 (1994).
[47] M.J. Frisch, G.W. Trucks, H.B. Schlegel, G.E. Scuseria, M.A. Robb, J.R. Cheeseman, J.A. Montgomery Jr, T. Vreven, K.N. Kudin, J.C. Burant, J.M. Millam, S.S. Iyengar, J. Tomasi, V. Barone, B. Mennucci, M. Cossi, G. Scalmani, N. Rega, G.A. Petersson, H. Nakatsuji, M. Hada, M. Ehara, K. Toyota, R. Fukuda, J. Hasegawa, M. Ishida, T. Nakajima, Y. Honda, O. Kitao, H. Nakai, M. Klene, X. Li, J.E. Knox, H.P. Hratchian, J.B. Cross, V. Bakken, C. Adamo, J. Jaramillo, R. Gomperts, R.E. Stratmann, O.Yazyev, A.J. Austin, R. Cammi, C. Pomelli, J.W. Ochterski, P.Y. Ayala, K. Morokuma, G.A. Voth, P. Salvador, J.J. Dannenberg, V.G. Zakrzewski, S. Dapprich, A.D. Daniels, M.C. Strain, O. Farkas, D.K. Malick, A.D. Rabuck, K. Raghavachari, J.B. Foresman, J.V. Ortiz, Q. Cui, A.G. Baboul, S. Clifford, J. Cioslowski, B.B. Stefanov, G. Liu, A. Liashenko, P. Piskorz, I. Komaromi, R.L. Martin, D.J. Fox, T. Keith, M.A. Al-Laham, C.Y. Peng, A. Nanayakkara, M. Challacombe, P.M.W. Gill, B. Johnson, W. Chen, M.W. Wong, C. Gonzalez, and J.A. Pople, *Gaussian 03, Revision E.01* (Gaussian, Inc., Wallingford CT, 2004).
[48] P. Perdew, J.A. Chevary, S.H. Vosko, K.A. Jackson, M.R. Pederson, D.J. Singh and C. Fiolhais, Phys Rev B **46**, 6671 (1992).
[49] P.J. Hay and W.R. Wadt, J. Chem. Phys. **82**, 270 (1985).
[50] W.R. Wadt and P.J. Hay, J. Chem. Phys. **82**, 284 (1985).
[51] P.J. Hay and W.R. Wadt, J. Chem. Phys. **82**, 299 (1985).

[52] R. Krishnan, J.S. Binkley, R. Seeger and J.A. Pople, J. Chem. Phys. **72**, 650 (1980).
[53] W.J. Hehre, L. Radom, P. V. R Schleyer and J. A Pople, *Ab Initio Molecular Orbital Theory* (Wiley, New York, 1986).
[54] T.B. Tai, P.V. Nhat, M.T. Nguyen, S. g. Li and D.A. Dixon, J. Phys. Chem. A **115**, 7673 (2011).
[55] I. Boustani, W. Pewestort, P. Fantucci, V. Bonacic-Koutecky and Koutecky, J. Phys. Rev. B **35**, 9437 (1987).
[56] R.O. Jones, A.I. Lichtenstein and J. Hutter, J. Chem. Phys. **106**, 4566 (1997).
[57] K. Rao, S.N. Khanna and P. Jena, Phys. Rev. B **43**, 1416 (1991).
[58] A.D. Becke and K.E. Edgecombe, J. Chem. Phys. **92**, 5397 (1990).